Molecular Biology of the Cell
Vol. 20, 5276–5289, December 15, 2009

The CORVET Subunit Vps8 Cooperates with the Rab5 Homolog Vps21 to Induce Clustering of Late Endosomal Compartments

Daniel F. Markgraf,*† Franziska Ahnert,*‡ Henning Arlt,*‡ Muriel Mari,‡§ Karolina Peplowska,*‖ Nadine Epp,* Janice Griffith,§ Fulvio Reggiori,§ and Christian Ungermann*

*University of Osnabrück, Department of Biology, Biochemistry Section, 49076 Osnabrück, Germany; and §University Medical Centre Utrecht, Department of Cell Biology, and Institute of Biomembranes, 3584 CX Utrecht, The Netherlands

Submitted June 24, 2009; Revised September 11, 2009; Accepted October 6, 2009
Monitoring Editor: Patrick J. Brennwald

Membrane tethering, the process of mediating the first contact between membranes destined for fusion, requires specialized multisubunit protein complexes and Rab GTPases. In the yeast endolysosomal system, the hexameric HOPS tethering complex cooperates with the Rab7 homolog Ypt7 to promote homotypic fusion at the vacuole, whereas the recently identified homologous CORVET complex acts at the level of late endosomes. Here, we have further functionally characterized the CORVET-specific subunit Vps8 and its relationship to the remaining subunits using an in vivo approach that allows the monitoring of late endosome biogenesis. In particular, our results indicate that Vps8 interacts and cooperates with the activated Rab5 homolog Vps21 to induce the clustering of late endosomal membranes, indicating that Vps8 is the effector subunit of the CORVET complex. This clustering, however, requires Vps3, Vps16, and Vps33 but not the remaining CORVET subunits. These data thus suggest that the CORVET complex is built of subunits with distinct activities and potentially, their sequential assembly could regulate tethering and successive fusion at the late endosomes.

INTRODUCTION

Eukaryotic cells contain a highly dynamic endomembrane system, in which individual organelles retain their identity despite continuous vesicle generation and fusion. Vesicles that bud from a donor membrane are targeted and delivered to each individual organelle, where they release their cargo after fusion with the acceptor membrane. A first layer of specificity for the fusion reaction is provided by tethering factors that can be grouped into long rod-shaped monomeric proteins, such as EEA1 and p115/Uso1, and multisubunit tethering complexes (Whyte and Munro, 2002). Tethers act in concert with small monomeric Rab and Arf GTPases (Drin *et al.*, 2008). In the case of the long tether GMAP210, it has recently been shown that the cooperation of a membrane curvature sensing motif and an Arf1-binding site positioned at opposite ends of the protein can trigger tethering in vitro (Drin *et al.*, 2008). The analysis of the tethering function of multimeric complexes, in contrast, has been scarce so far. Nevertheless, specific multisubunit tethering complexes and Rab GTPases have been assigned to each organelle of the endomembrane system highlighting their crucial relevance. At the Golgi, the TRAPP complex cooperates with Rab1/Ypt1 (Wang *et al.*, 2000), whereas the GARP complex and the Rab Ypt6 are required for endosome-to-Golgi transport (Conibear *et al.*, 2003), and the Dsl-complex and Ypt1 are necessary for ER-to-Golgi transport (Kraynack *et al.*, 2005; Kamena *et al.*, 2008). The exocyst together with the Rab Sec4, on the other hand, is required for delivery of Golgi-derived vesicles to the plasma membrane (Grosshans *et al.*, 2006). In addition, two sets of Rab GTPases and tethering complexes are involved in endosomal trafficking to the lysosome/vacuole.

The vacuole represents the main degradative organelle in yeast. As a result, this compartment is the terminal station of numerous transport routes including the cytosol-to-vacuole transport pathway, autophagy, the AP-3 pathway (a direct route from the *trans*-Golgi network), the carboxypeptidase Y (CPY) pathway, and the endocytic pathway. Endosomal transport occurs via the maturation of early endosomes (EE) into late endosomes (LE). In particular, LE form intraluminal vesicles and the resulting multivesicular bodies (MVBs) fuse with the vacuole to release their cargoes. During this process, the retromer complex seems to be recruited via Rab7 (Rojas *et al.*, 2008; Seaman *et al.*, 2009), presumably to promote retrieval of cargo receptors from maturing MVBs. In yeast, retromer is responsible to retrieve the cargo receptor Vps10, which delivers CPY to the LE (Burda *et al.*, 2002).

The first membrane contact during the fusion reaction at the vacuole is mediated by the vacuolar HOPS (homotypic fusion and vacuole protein sorting) tethering complex and the yeast Rab7 homolog Ypt7 (Ostrowicz *et al.*, 2008; Nickerson *et al.*,

This article was published online ahead of print in *MBC in Press* (http://www.molbiolcell.org/cgi/doi/10.1091/mbc.E09–06–0521) on October 14, 2009.

‡ These authors contributed equally to this work.

Present addresses: †Harvard Medical School, Boston, MA 02115; ‖Max-Planck Institute of Biochemistry, 82152 Martinsried, Germany.

Address correspondence to: Christian Ungermann (christian.ungermann@biologie.uni-biologie.de) or Fulvio Reggiori (F.Reggiori@umcutrecht.nl).

2009). The HOPS complex consists of four Vps proteins (Vps11, Vps16, Vps18, and Vps33) forming the class C core and two additional subunits, Vam6/Vps39 and Vam2/Vps41 (Price *et al.*, 2000a,b). Vam6/Vps39 has guanine nucleotide exchange factor (GEF) activity and converts Ypt7-GDP into its GTP-bound form (Wurmser *et al.*, 2000). Activated Ypt7 is able to bind the whole HOPS complex, revealing the role of the latter as a specific Ypt7 effector. Recent data suggest that the Vps41 subunit, which is regulated by the casein kinase Yck3 (Lagrassa and Ungermann, 2005; Cabrera *et al.*, 2009), is the direct effector of Ypt7-GTP (Brett *et al.*, 2008; Cabrera *et al.*, 2009). The endosomal tethering complex CORVET (class C core vacuole/endosome tethering) has a striking similarity to the HOPS complex (Peplowska *et al.*, 2007; Nickerson *et al.*, 2009). It shares the class C core, but Vam6/Vps39 and Vam2/Vps41 are replaced by the homologous proteins Vps3 and Vps8, respectively. The Rab5 homolog Vps21 is involved in the early steps of the endocytic pathway (Peterson *et al.*, 1999; Gerrard *et al.*, 2000) and interacts with the CORVET complex (Peplowska *et al.*, 2007), thereby mirroring the tethering machinery at the vacuole. It has previously been shown that Vps21 is required for the membrane association of the CORVET complex subunit Vps8, a peripheral membrane protein necessary for transport between Golgi and endosomes (Horazdovsky *et al.*, 1996). It has also been observed that overexpression of Vps21 leads to some accumulation of structures positive for the LE SNARE Pep12 and endocytosed cargoes (Gerrard *et al.*, 2000).

In this study, we have investigated the functional relationship between Vps21, Vps8, and the remaining CORVET complex subunits in the context of LE tethering. We demonstrate that Vps8 cooperates with Vps21-GTP to mediate endosomal clustering in a reaction that is dependent on Vps3. Vps8 is the only CORVET subunit that is enriched on LE under these conditions, suggesting that it is a marker for the maturation of LE.

MATERIALS AND METHODS

Yeast Strains and Plasmids

Strains used are listed in Supplemental Table S1. Gene deletion and tagging was done by homologous recombination of PCR fragments. Vps41, Vps39, Vps3, Vps21, and Cps1 were genomically tagged at the N-terminus using an *URA3-PHO5-GFP-MYC* cassette amplified from the plasmid pGL (a kind gift from Sean Munro, MRC, Cambridge, United Kingdom). *VPS8* was placed under the control of the *GAL1*-promoter using a PCR fragment containing flanking regions of the *VPS8* gene, amplified from pFA6a-*HIS3MX6-GAL1-3xHA*, pFA6a-*TRP1-PGAL1-3HA*, or pFA6a-*HIS3MX6-PGAL1-GFP* as template (Longtine *et al.*, 1998). Mnn9 was tagged with tdTomato variant of red fluorescent protein (RFP) using PCR fragments containing flanking regions of the *MNN9* gene, amplified from *pFA6a-td-Tomato-KanMX6* (kindly provided by Michael Knop, EMBL Heidelberg, Germany). The *ADH1* and *TEF1* promoters with or without *GFP* inserts were cloned in front of *VPS21* and *VPS8* by amplifying PCR products from pYM-N7, pYM-N9, or pYM-N19 plasmids that contain flanking regions of the respective genes (Janke *et al.*, 2004). Vps3 was C-terminally tagged with the tandem affinity purification (TAP) tag using a *TAP-URA3* cassette amplified from plasmid pBS1539 (Puig *et al.*, 1998), and Vps10 was C-terminally tagged using a *GFP-TRP1* cassette as a template (Longtine *et al.*, 1998). The plasmid carrying green fluorescent protein (GFP)-tagged Ste3 was kindly provided by Jeffrey Gerst (Weizman Institute of Science, Rehovot, Israel). To generate the RFP-tagged versions of Pep12, Vam3, and Vps21, genes were amplified from genomic DNA, digested with BamHI/SacI and inserted into BamHI/SacI site of the pV2 plasmid that carries DsRed from pRSET-B DsRed dimer (provided by S. Munro). Y2H analyses were conducted using the pACT2 (CLONTECH Laboratories) and pFBT9 (a modified pGBT9 vector from CLONTECH Laboratories) vectors (provided by F. Barr, University of Liverpool, Liverpool, United Kingdom). Genes of interest were amplified from genomic DNA, and after digestion with BamHI/XhoI, they were ligated into pACT2 or into a BamHI/SalI site of pFBT9. Mutant versions of *VPS21*, *YPT7*, *YPT52*, and *YPT53* were generated by first cloning wild-type genes into pGEX4T3 vector followed by site-directed mutagenesis using the quick-change mutagenesis kit (Stratagene Europe, Amsterdam, the Netherlands). Point-mutated Rab was amplified from these vectors and cloned into pACT2 and pFBT9 as described above. All inserts and mutations were confirmed by sequencing. The generation of the all-*GAL1* CORVET strain will be reported elsewhere (F. Ahnert and C. Ungermann, unpublished data).

Yeast Cell Lysis

After overnight growth in rich medium containing 2% glucose (YPD) or 2% galactose (YPG), cell cultures were diluted to OD_{600} = 0.5 and incubated for 2 h in 30°C. Cells (50 OD_{600} units) were collected, washed once with dithiothreitol (DTT) buffer (10 mM DTT, 0.1 M Tris/HCl, pH 9.4), resuspended in 1 ml of DTT buffer, and incubated for 10 min in 30°C. Cells were then centrifuged (2 min, 4620 × *g*), resuspended in 300 μl of spheroplasting buffer (0.16 × YPD, 50 μM KPi buffer, pH 7.4, and 0.6 M sorbitol), and incubated for 20 min at 30°C in the presence of lyticase. Spheroplasts were finally centrifuged for 3 min at 1530 × *g*, the pellet was resuspended in 1 ml of lysis buffer (0.2 M sorbitol, 150 mM KCl, 20 mM HEPES/KOH, pH 6.8, 1 mM DTT, 1 mM PMSF, 0.1 μg/ml leupeptin, 1 mM *o*-phenanthroline, 0.5 μg/ml pepstatin, and 0.1 mM pefablock) supplemented with 6 μl of 0.4 mg/ml DEAE dextran, and incubated for 5 min on ice. Samples were briefly heat-shocked (2 min, 30°C), and cell debris was removed by centrifugation at 300 × *g* for 3 min. The cell lysates were used for further experiments.

Biochemical Fractionation of Yeast Cells

Fractionation was done as described (Lagrassa and Ungermann, 2005). Briefly, yeast cell lysates were prepared and centrifuged for 15 min at 13,000 × *g* at 4°C. The supernatant was centrifuged for 1 h at 100,000 × *g*, resulting in a P100 pellet and a S100 supernatant fraction. The S100 fraction was trichloroacetic acid (TCA)-precipitated, acetone-washed, and, as the P13 and P100 pellet fractions, resuspended in SDS sample buffer. Proteins were analyzed by SDS-PAGE and Western blotting.

Fluorescence Microscopy

Cell staining with the lipophilic dye FM4-64 was done as previously described (Lagrassa and Ungermann, 2005). For fluorescence microscopy of cells carrying GFP- and RFP-tagged proteins, cells were grown to logarithmic phase in YPD or selective medium, collected by centrifugation, and washed once with 1 ml of PBS buffer before imaging. To follow Ste3-GFP sorting, cycloheximide (3,125 μg/ml) was added to cells. After a 45-min incubation, cells were washed twice and analyzed by fluorescence microscopy. Images were acquired using a Leica DM5500 microscope (Leica, Mannheim, Germany) equipped with a SPOT Pursuit-XS camera using filters for GFP, FM4-64, and RFP, and DAPI. The pictures were processed using Adobe Photoshop 7 (Adobe Systems, Munich, Germany).

Total Protein Extraction from Yeast

Protein extracts were obtained from the indicated strains by alkaline lysis. One OD_{600} unit of yeast cells was lysed in 0.25 M NaOH, 140 mM β-mercaptoethanol, and 3 mM PMSF. After a 10-min incubation on ice, samples were subjected to TCA precipitation followed by a wash with acetone. SDS sample buffer was added and equal amounts of protein extracts were analyzed by SDS-PAGE and Western blotting.

Glutathione-Rab Pulldown

Recombinant glutathione *S*-transferase (GST) fusion proteins (350 μg per sample) obtained from *E. coli* were incubated with 500 μl of 20 mM HEPES/NaOH (pH 7.4), 20 mM EDTA and 10 mM GDP or GTPγS. After incubation at 30°C for 15 min, samples were adjusted to 25 mM $MgCl_2$ and loaded onto 50 μl of prewashed GSH beads. After incubation for 1 h at 4°C, GDP and GTPγS-loaded Rabs were resuspended in 200 μl buffer A (20 mM HEPES/NaOH, pH 7.4, 100 mM NaCl, and 1 mM $MgCl_2$) and 10 mM GDP or GTPγS, respectively. Eighty OD_{600} equivalents of cells were washed once in buffer A and resuspended in 300 μl of this buffer. Glass beads were added, and samples were extensively vortexed for 5 min at 4°C. After centrifugation (5 min, 300 × *g*), the supernatant was kept on ice, and vortexing was repeated in an additional 300 μl of buffer A. Supernatants were combined and adjusted to 1% TX-100. After incubation for 20 min at 4°C, samples were centrifuged for 10 min at 20,000 × *g* and the resulting supernatant was applied to GSH-bound Rabs. Beads were finally incubated for 1 h at 4°C on a rotating wheel, washed three times with decreasing TX-100 concentrations, and eluted by incubation in 20 mM HEPES/NaOH, pH 7.4, 200 mM NaCl, 20 mM EDTA, and 0.1% TX-100 for 20 min at room temperature. Eluates were TCA-precipitated and analyzed by SDS-PAGE followed by Western blotting.

TAP Purification (Mini-Scale)

TAP-tag protein purification was performed as described (Peplowska *et al.*, 2007). In brief, yeast cell lysates were prepared from 500 OD_{600} equivalents of cells using lysis buffer (50 mM HEPES/KOH, pH 7.4, 300 mM NaCl, 0.15% NP-40 [Igepal CA-630; Sigma-Aldrich, Munich, Germany], and 1.5 mM $MgCl_2$), followed by a centrifugation at 20,000 × *g* at 4°C. The supernatant

was centrifuged for 1 h at 1000,000 × *g*, and the cleared lysate was loaded onto prewashed IgG beads. After 1 h of incubation at 4°C, the beads were washed twice with lysis buffer. Bound proteins were eluted by boiling the beads for 4 min in 20 μl Laemmli buffer and analyzed by SDS-PAGE and Western blotting.

Yeast Two-Hybrid Assay

Yeast two-hybrid assays (Y2Hs) were carried out as described (Shorter *et al.*, 1999). Combinations of pACT2- and pFBT9-Y2H vectors carrying the DNA sequence of the indicated proteins were transformed into the yeast strain PJ69-4A and plated onto synthetic media lacking leucine and tryptophan (double dropout [DDO]). Transformants were successively transferred first onto medium lacking leucine, tryptophan, histidine, and adenine (quadruple dropout [QDO]) and afterward on DDO medium containing 2% glucose. For each Y2H-vector combination, four clones were analyzed. An interaction between tested proteins results in the capability to grow on QDO medium.

CPY Spot Assay

After overnight growth in glucose-(YPD) or galactose-(YPG) containing medium, cells were diluted to 1, 0.1, and 0.01 OD_{600}, and 5 μl of each dilution was spotted on YPD or YPG medium plates. Plates were incubated overnight at 30°C and replica-plated onto nitrocellulose filters that were placed on fresh YPD or YPG plates. After incubation at 30°C overnight, filters were removed, thoroughly washed, and further processed according to a standard Western blotting protocol. Secreted CPY was detected by decorating filters with anti-CPY antibody.

Electron Microscopy and Immunoelectron Microscopy Analyses

Strains were grown to exponential phase before being processed for electron microscopy (EM). Permanganate fixation, dehydration and embedding in the Spurr's resin, and immunogold labeling of cryosections were carried out as described (Griffith *et al.*, 2008). Sections were viewed in a Jeol 1200 transmission electron microscope (Jeol, Tokyo, Japan), and images were recorded on Kodak 4489 sheet films (Eastman Kodak, Rochester, NY).

RESULTS

Vps21 Accumulation in a LE Compartment

The study of the HOPS complex molecular function at the vacuole has been facilitated by available enzymatic and visual fusion assays (Ostrowicz *et al.*, 2008). In contrast, there are no comparable assays to investigate the role of the homologous CORVET complex in tethering and fusion at the LE and its interrelationship with its Rab partner, the Rab5 homolog Vps21. In previous studies, we noticed that overexpression of Vps8 leads to the formation of what appears to be an enlarged, perinuclear Vps21-positive organelle (Peplowska *et al.*, 2007), hereafter called the Vps21 compartment. The prominence of this structure correlates with Vps8 cellular levels as shown by driving Vps8 expression from either the *GAL1* (Supplemental Figure S1, A, B, and D) or the *TEF1* promoter (Supplemental Figure S1, E and F). The Vps21 compartment can also be observed when Vps21 is overproduced (Gerrard *et al.*, 2000). Additionally, co-overexpression of Vps21 and Vps8 had cumulative effects. Placing the GFP-Vps21 fusion protein under the control of the *PHO5*, the *ADH1* (Supplemental Figure S1) or the *GAL1* promoter (see Figure 7C) revealed that the expression levels of Vps21 influence the size of the Vps21 compartment (Supplemental Figure S1, D and E). Importantly, the deletion of the CORVET subunit *VPS3* results in the dissolution of the Vps21 compartment (Peplowska *et al.*, 2007). As a consequence, the Vps21 compartment does not seem to be just an aberration but rather an enlarged functional organelle that we thought could be exploited to visually investigate the CORVET complex functions at the LE in vivo. Before using its formation as an assay in our study, however, we made additional verifications.

First, we established that the Vps21-positive punctate structures induced by the Vps8 and the Vps21 overexpression are the same by colocalizing Vps21 and overproduced Vps8 in the wild-type background (Figure 1B). Second, we confirmed that the Vps21 compartment is an endocytic structure by labeling it with the lipophilic dye FM4-64 (Figure 1A). Third, we colocalized GFP-Vps21 with endosomal and vacuolar protein markers to show that these organelles are indeed LE. Although an RFP-tagged version of the LE SNARE Pep12 was clearly enriched in the Vps21 compartments (Figure 1C), the localization of the RFP-tagged vacuolar SNARE Vam3 (Figure 1D), the Golgi-resident protein Mnn9 (Figure 1E), or the EE protein marker Vac1 (Figure 1F) was not affected by Vps8 up-regulation. Fourth, to place the Vps21 compartment in a more defined trafficking step of the endosomal route to the vacuole, we compared the localization of GFP-Vps21 in wild-type cells to that in class D *vps* mutants (Raymond *et al.*, 1992). Most of the class D Vps proteins, including the Vps21 GEF Vps9, the Sec1-like protein Vps45, and the SNARE Pep12 are implicated in vesicle fusion at the EE. Their deletion leads to an enlarged vacuole but also to the accumulation of small vesicles with a 40-nm diameter throughout the cytoplasm that are unable to fuse with LE (Cowles *et al.*, 1994; Becherer *et al.*, 1996; Burd *et al.*, 1996). In agreement with this, endocytic and biosynthetic cargo protein sorting is blocked. When we analyzed GFP-Vps21 localization in *vps9*Δ, *vps45*Δ, and *pep12*Δ mutants, we observed an accumulation of Vps21 (Figure 1G) similar, though weaker, to the strong accumulation of GFP-Vps21 upon overexpression of Vps8 (Figure 1A, Supplemental Figure S1). Vps21 clustering was slightly enhanced when Vps8 was overexpressed in the same backgrounds (Figure 1H). This indicates that the Vps21 compartment is indeed a LE compartment that can form independently of EE factors. Finally, we demonstrated that the formation of the Vps21-compartment is due to changes in LE organization rather than an aberrant accumulation of membranes of various origins, because the subcellular distribution of Vps21 and Vps8 was not affected by Vps8 overexpression as assessed by subcellular fractionation (Figure 1I).

Taken all these data together, we concluded that the Vps21 compartment is an enlarged organelle with LE characteristics. Therefore its formation induced by the dual overexpression of Vps21 and Vps8 can be used as a read-out to unravel the interplay of CORVET subunits.

The Vps21 Compartment Is Formed by Clustered MVBs

The similar effect on Vps21 localization upon class D gene deletion or Vps8 overexpression prompted us to ask whether the Vps21-compartment is formed by the accumulation of vesicular structures. To address this question, we analyzed wild-type and Vps8–overexpressing cells in the presence of up-regulated Vps21 by EM (Figure 2, A–H). Vps8 was placed under the control of the strong *TEF1* promoter in the SEY6210 wild-type strain, which was used for these EM analyses. Although the expression levels of Vps8 driven by the *TEF1* promoter were lower compared with those when Vps8 is under the control of the *GAL1* promoter (Figure 2I), GFP-Vps21 was still primarily accumulating in a single bright dot adjacent to the vacuole (Figure 2K). Cells expressing GFP-Vps21 alone (Figure 2A) were ultrastructurally identical to the untransformed wild-type strain (not shown). In contrast, overproduction of Vps8 led to two evident morphological phenotypes. First, it was much easier to detect vesicular structures in the cytoplasm (Figure 2B, arrowhead). Those were of two types: most were electron-dense vesicles with a diameter of ~80–100 nm (Figure 2B), whereas a minority were vesicular organelles with a distinct limiting membrane. Second, the 80–100-nm vesicles were also detected clustered together adjacently to the vacuole

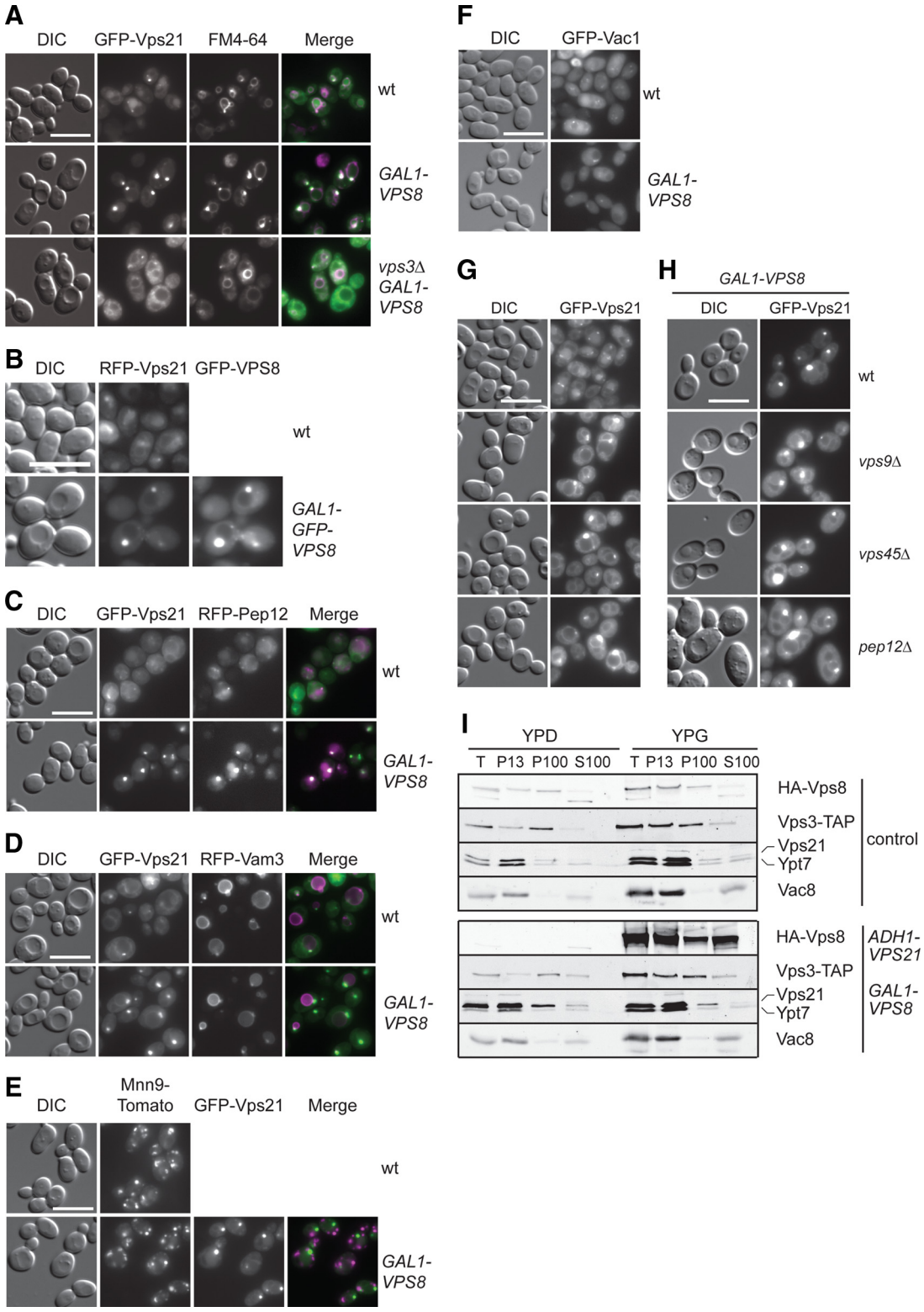

Figure 1. The Vps21-compartment resembles an endosomal structure. (A) Localization of GFP-Vps21 in the absence of *VPS3*. Wild-type and Vps8-overexpressing cells in the presence or absence of *VPS3* were grown to logarithmic phase in YPG medium, stained with FM4-64, harvested, washed once with PBS buffer, and analyzed by fluorescence microscopy. Size bar, 10 μm. (B) Colocalization of RFP-Vps21 and overexpressed GFP-Vps8. The top panel shows the localization of RFP-Vps21 in the wild-type background. In the bottom panel, RFP-Vps21 and GFP-Vps8 (*PHO5-RFP-Vps21 GAL1-GFP-VPS8*) were coexpressed in wild-type cells. Cells were analyzed by fluorescence microscopy as described in A. Size bar, 10 μm. (C–F) Colocalization of Vps21 with different organelle protein markers after Vps8 overproduction. RFP-Pep12 (C), RFP-Vam3 (D), or Mnn9-Tomato (E) were coexpressed with GFP-Vps21 in wild-type and Vps8-overexpressing cells and visualized by fluorescence microscopy. In F, GFP-tagged Vac1 was localized in both cell types. Microscopy analysis was performed as in A. (G and H) Localization of GFP-Vps21 in the indicated class D *vps* mutant strains in absence (G) or presence (H) of overexpressed Vps8. The cells were

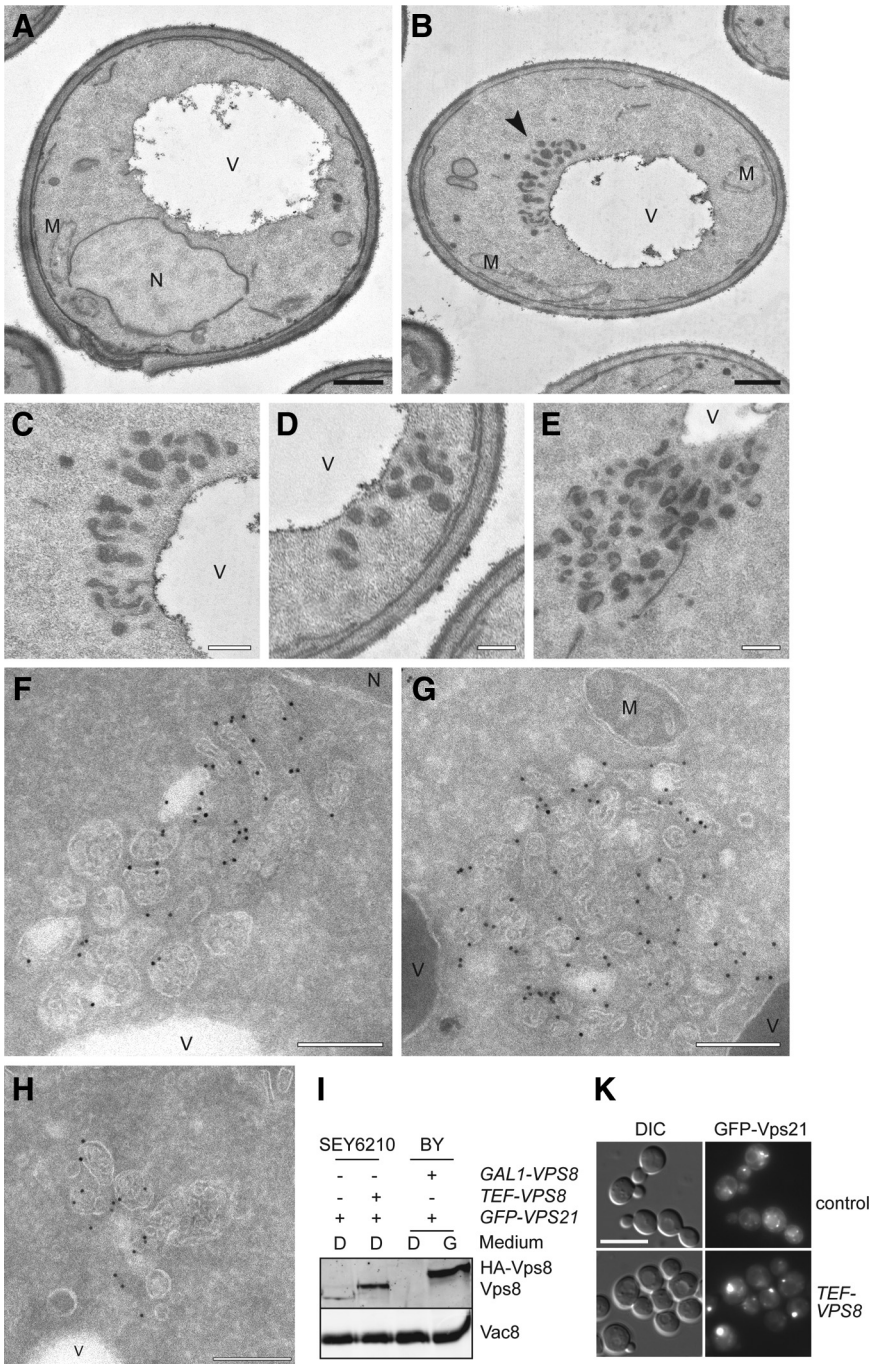

Figure 2. Ultrastructural analysis reveals the clustering of LE structures. (A–H) Ultrastructural analyses. The SEY6210 *PHO5-GFP-VPS21* (A), SEY6210 *PHO5-GFP-VPS21 TEF1-VPS8* (B–E), SEY6210 *TEF1-GFP-VPS8 ADH1-VPS21* (F and G), and *SEY6210 PHO5-GFP-VPS21 TEF1-HA-VPS8* (H) strains were grown to exponential phase and embedded in Spurr's resin (A–E) or prepared for IEM (F–H) as described in *Material and Methods.* Cryosections (F–H) were first incubated with goat anti-GFP antibodies (Rockland, Gilbertsville, PA) and then with 15-nm gold particles conjugated to protein A. Arrowheads in B indicate the abnormal structures observed in those cells. (C to E) The clusters of vesicles observed in cells overexpressing Vps8. Clusters of small MVBs were observed in proximity of the vacuole limiting membrane. V, vacuole; M, mitochondrion; N, nucleus. Black bar, 500 nm; white bar, 200 nm. (I) Protein expression levels. P13 fractions obtained from cells grown in glucose- or galactose-containing medium were analyzed by separating equal amounts of proteins by SDS-PAGE and by decorating Western blots with antibodies recognizing Vps8 and Vac8 (loading control). (K) Formation of the Vps21 compartment in the SEY6210 strain background upon Vps8 overproduction. Localization of GFP-Vps21 in wild-type and *TEF1* promoter driven HA-tagged Vps8-expressing cells. Samples were analyzed by fluorescence microscopy as described in Figure 1A. Size bar, 10 μm.

(Figures 2, C–E). Consequently, these clusters of vesicles, with a diameter of ~400–500 nm, very likely represent the perivacuolar Vps21 compartment imaged by fluorescence microscopy (e.g., Figure 1A). The close proximity of the vesicles to each other suggests that these structures could correspond to tethered LE.

To determine the distribution of GFP-Vps8 within these structures, cells were analyzed by immuno-EM (IEM) using anti-GFP antibodies (Figure 2, F and G). This led to a striking observation: Vps8 is found on the surface of clustered MVBs, appearing to be mostly concentrated at the contact interfaces. Similar observations were made for Vps21 when tagged with GFP (Figure 2H). These structures are heterogeneous in form and size, and they were always observed in close proximity to vacuole and thus very likely represent

Figure 1 (cont). analyzed by fluorescence microscopy as in A. Size bar, 10 μm. (I) Subcellular distribution of CORVET and endolysosomal Rab GTPases. Lysed spheroplasts from cells expressing C-terminally TAP-tagged Vps3 and HA-tagged Vps8 (control) or from cells overexpressing Vps21 and Vps8 (*ADH-VPS21 GAL1-HA-VPS8*) were subjected to two differential centrifugations, resulting in a 13,000 $\times$ *g* pellet (P13), a 100,000 $\times$ *g* pellet (P100), and a final supernatant (S100). Fractions were analyzed by Western blotting using antibodies against the indicated proteins.

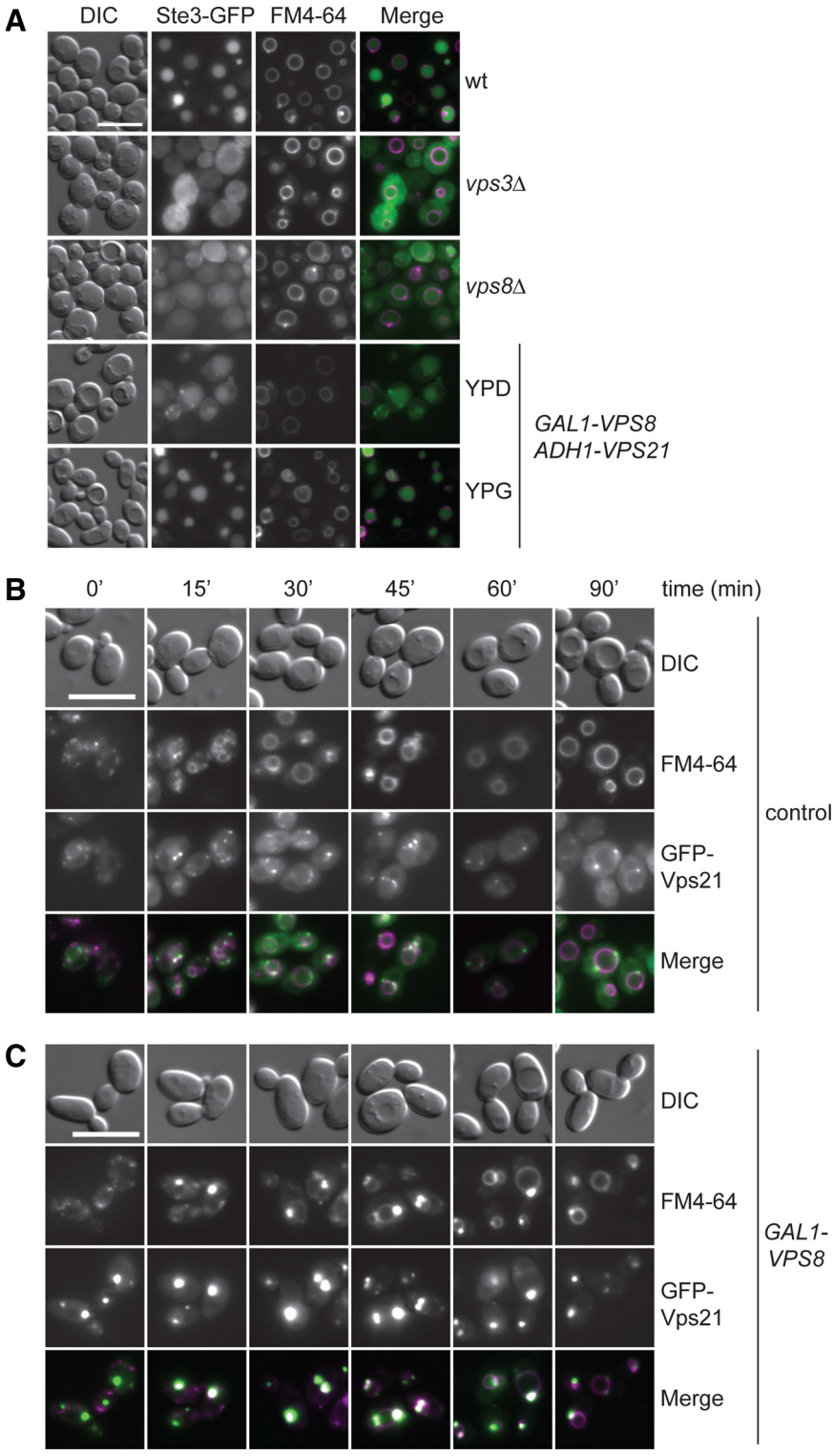

Figure 3. Sorting of CPY and endocytic cargoes upon Vps8 overproduction. (A) Sorting of an endocytosed receptor. Localization of Ste3-GFP was determined in wild-type, *vps3*Δ, *vps8*Δ, and Vps8– and Vps21–co-overexpressing (*GAL1-VPS8*, *ADH1-VPS21*) cells by fluorescence microscopy after vacuole staining with FM4-64 and cycloheximide treatment. Ste3-GFP, which is sorted into the vacuole lumen in wild-type cells, is mislocalized in *vps3*Δ and in *vps8*Δ cells, consistent with a role of both proteins along the endocytic pathway. Size bar, 10 μm. (B and C) Time-course internalization of FM4-64. Wild-type (B) and Vps8– and Vps21–co-overexpressing (*GAL1-VPS8*, *ADH1-GFP-VPS21*; C) cells were incubated for 2 min at 30°C with FM4-64, chased for the indicated times, and analyzed by fluorescence microscopy as in Figure 1A.

the clusters of vesicles observed by conventional EM. Even though conditions have been reported that lead to the enrichment of MVBs (Lazar *et al.*, 2002; Pons *et al.*, 2008), we are not aware that such an accumulation of MVBs has been reported by any previous study.

Cargo Sorting through the Vps21 Compartment

We were wondering if the enhanced clustering of Vps21-positive LE upon Vps8 overproduction would affect transport to the vacuole. To test this, we analyzed the trafficking of endocytic and biosynthetic cargoes. Sorting into the vacuole lumen via MVBs is not affected by the formation of the Vps21 compartment, because GFP-tagged Ste3 and Cps1

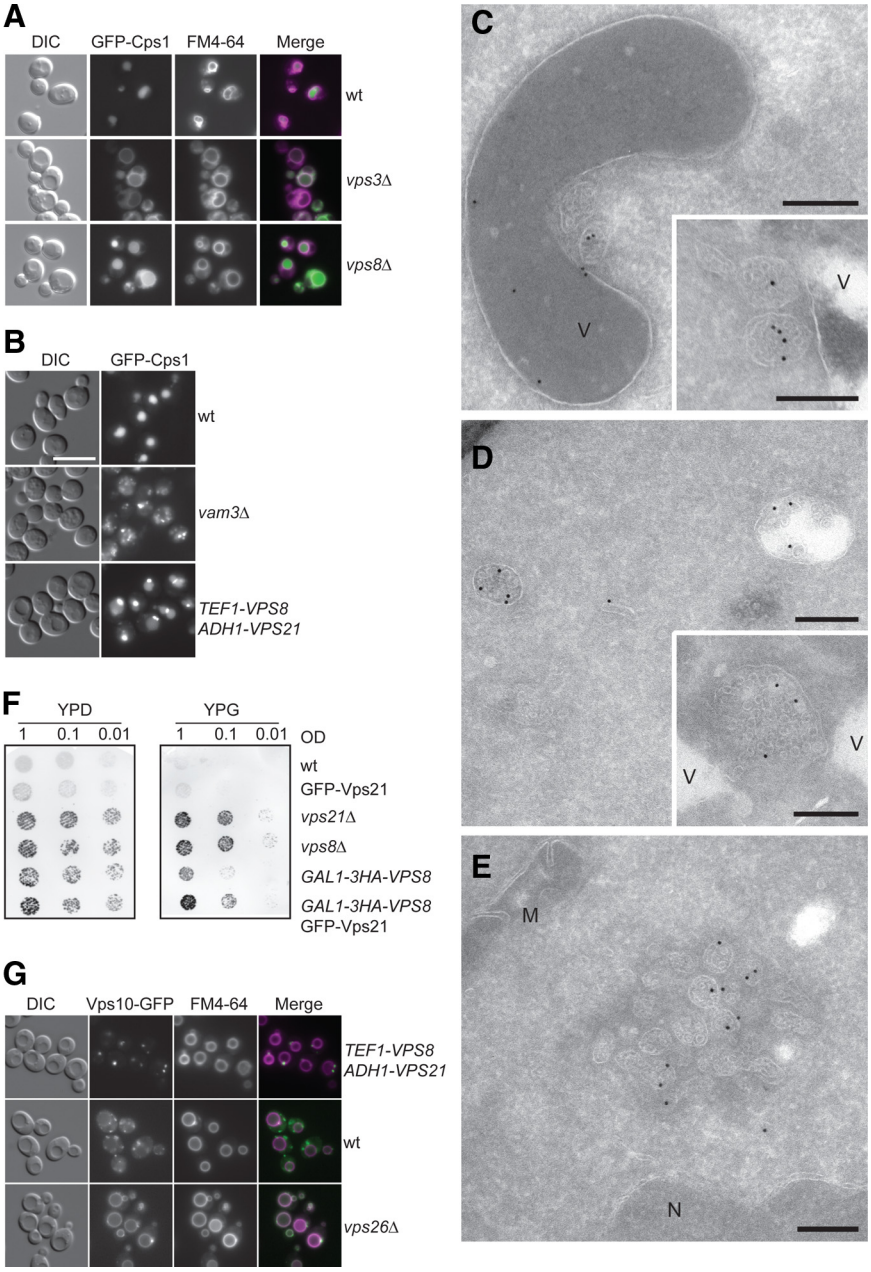

Figure 4. Localization of MVB-cargo within the Vps21 compartment. (A) Sorting of a biosynthetic cargo. GFP-Cps1 was expressed in wild-type, *vps3*Δ, or *vps8*Δ strains, and cells were stained with FM4-64 before being analyzed by fluorescence microscopy as described in Figure 1A. As Ste3-GFP (Figure 3A), GFP-Cps1 is affected by the deletions of *VPS3* and *VPS8*. (B) Sorting of biosynthetic cargo. GFP-Cps1 was expressed in the SEY6210 wild-type, *vam3*Δ, or Vps8– and Vps21–co-overexpressing background. Fluorescence microscopy analysis was performed as in Figure 1. (C–E) Ultrastructural analyses. The strains used for fluorescence microscopy analysis in B, SEY6210 *PHO5-GFP-CPS1* (C), SEY6210 *PHO5-GFP-CPS1 vam3*Δ (D), and SEY6210 *PHO5-GFP-CPS1 TEF1-VPS8 ADH1-VPS21* (E), were grown to exponential phase and prepared for IEM as described in Figure 2. Cryosections were incubated with rabbit anti-GFP antibodies (Abcam, Cambridge, United Kingdom) and then with 15-nm gold particles conjugated to protein A. V, vacuole; M, mitochondrion; N, nucleus; Black bar, 200 nm. (F) CPY missorting analysis. The indicated strains were spotted on either a glucose- (YPD) or a galactose- (YPG) containing plate. After incubation at 30°C for 1 d, plates were replica-plated onto nitrocellulose filters, which were then transferred again on the top of a new YPD or YPG plate. Filters were removed after an overnight incubation at 30°C and thoroughly washed with PBS buffer, and secreted CPY was detected by decorating filters with anti-CPY antibodies. (G) Sorting of Vps10. The indicated cells expressing C-terminally GFP-tagged Vps10 were processed for fluorescence microscopy as in Figure 1A.

where normally delivered to their final destination (Piper *et al.*, 1995; Odorizzi *et al.*, 1998; Figures 3A and 4B). In contrast, the trafficking of the same proteins is impaired in *vps3*Δ or *vps8*Δ deletion mutants (Figures 3A and 4A). To confirm that the endocytic cargoes are indeed transported via the Vps21 compartment, we also followed trafficking of the lipophilic dye FM4-64 from the plasma membrane to the vacuole via endosomes over time (Figure 3, B and C). Normal FM4-64 trafficking was observed in wild-type cells, as expected, and FM4-64 colocalized with GFP-Vps21 (e.g., endosomes, at early internalization time points; Figure 3B). When Vps8 is overproduced, even if with a slight slower transport rate, FM4-64 still reaches the vacuole, and importantly, this occurs passing through the Vps21 compartment (Figure 3C).

We then asked if we could detect cargo within the LE compartments. Even though the presence of the Vps21 compartment did not compromise the correct sorting of GFP-Cps1 into the vacuolar lumen, some GFP-Cps1 accumulated in distinct puncta adjacent to the vacuole (Figure 4B). These were identified to be tethered MVBs by IEM. In wild-type cells, only few MVBs were present, and GFP-Cps1 was found both in the MVB and the vacuole (Figure 4C). Previous studies have indicated that MVBs are accumulated in *vam3*Δ cells (Darsow *et al.*, 1997), and we could indeed detect GFP-Cps1 within these structures, which are not tethered together but scattered throughout the cytoplasm (Figure 4D). Importantly, the clustered MVBs observed upon co-overexpression of Vps8 and Vps21 also contain GFP-Cps1 (Figure 4E). These MVBs, however, are smaller in size, suggesting that the presence of Vps8 could affect the maturation and/or fusion of LE/MVBs. In contrast to sorting of GFP-Cps1, Ste3-GFP was not detected at the Vps21 compartment (Figure 3A). This could be due to the cycloheximide treatment

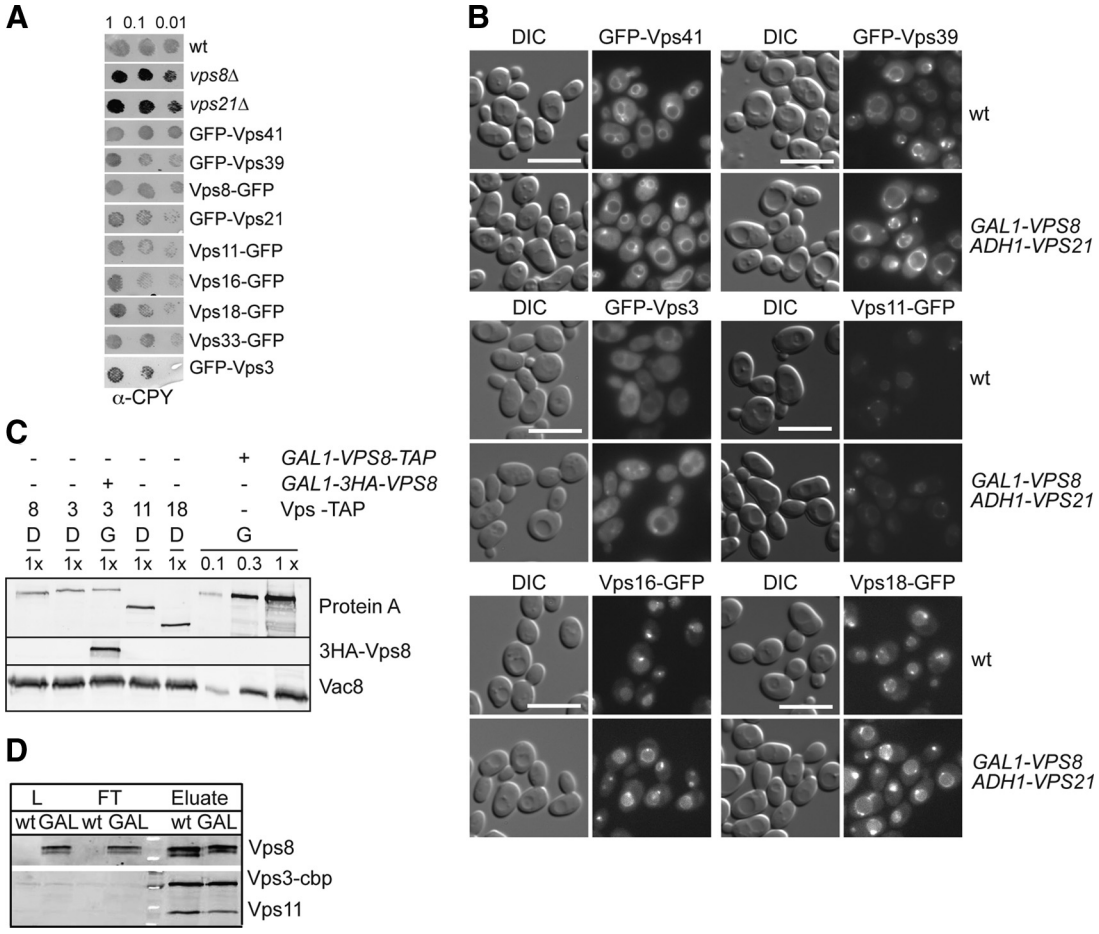

Figure 5. HOPS and CORVET subunit distribution on the Vps21 compartment. (A) CPY sorting. The indicated strains were spotted on YPD plates and analyzed as in Figure 4F. (B) Localization of GFP-tagged Vps41 and Vps39 (top), Vps3 and Vps11 (middle), and Vps16 and Vps18 (bottom) upon Vps8 overproduction. Fluorescence microscopy analysis was performed as in Figure 1A. (C) Relative expression levels of tagged CORVET subunits. Cells expressing the indicated TAP-tagged proteins were grown in glucose and galactose. Protein extracts were analyzed by SDS-PAGE followed by Western blotting. Extracts from *GAL1-VPS8-TAP* cells were loaded in the indicated dilutions to the gel. (D) CORVET assembly. C-terminally TAP-tagged Vps3 was purified form strains carrying HA-tagged Vps8 under the control of either the *VPS8* or the *GAL1* promoter using IgG beads. Load (L), flow-through (FT), and eluate were analyzed by SDS-PAGE and Western blotting using antibodies directed against Vps11, the calmodulin-binding peptide (cbp) or the HA tag.

of the cells during the sample preparation, which may allow Ste3 to pass through the tethered structures.

The accumulation of FM4-64 and Cps1 suggested a delay in the anterograde transport to the vacuole. To determine if other transport events in the endosomal system are impaired, we analyzed the missorting of CPY to the extracellular space using a plate assay. Although *vps21*Δ and *vps8*Δ mutants had an evident CPY secretion as expected, cells with up-regulated N-terminally tagged Vps21 behaved like the wild type (Figure 4F), consistently with the normal morphology observed by EM (Figure 2A). The overproduction of Vps8 alone resulted in a minor CPY secretion that was enhanced if combined with GFP-Vps21 up-regulation. Because CPY missorting is often caused by a trafficking defect of its sorting receptor Vps10, we analyzed the localization of Vps10, which is mostly found on endosomes in wild-type cells (Burda *et al.*, 2002; Figure 4G). In the absence of the retromer subunit Vps26, Vps10-GFP fails to be retrieved from endosomal compartments and ends on the vacuole surface (Burda *et al.*, 2002). Strikingly, Vps10-GFP accumulates strongly in one distinct perivacuolar dot reminiscent of the Vps21 compartment upon overproduction of Vps8 and Vps21 (Figure 4G).

Taken all together, our data show that up-regulation of Vps8 and the Rab5 GTPase Vps21 leads to an accumulation of MVBs that can sort cargoes into the vacuole lumen but accumulate the Vps10 receptor, presumably due to a delayed retromer function.

The CORVET Subunits Have Different Roles in the Tethering of the LE Membranes

Next, we decided to explore if the rest of the CORVET subunits plays a role in the tethering of the LE membranes. We first tested if their localization was altered in presence of a Vps21 compartment. The HOPS complex-specific subunits Vps39 and Vps41 were used as controls. Tagging of the subunit did not interfere with function as assessed by vacuole morphology (not shown) and CPY secretion (Figure 5A). The subcellular distribution of endogenously GFP-tagged Vps41, Vps39, Vps3, Vps11, Vps16, and Vps18, which was followed by fluorescence microscopy, was unaffected by the overproduction of Vps8 and Vps21 (Figure 5B). This observation could be explained by a function of Vps21 and Vps8 independently of the remaining CORVET subunits. For this reason, we then compared the expression

levels of the individual CORVET subunits. Wild-type cells express comparable levels of all CORVET subunits, whereas Vps8 is ~10-fold more abundant after overexpression (Figure 5C), and interestingly, our data show that it is the only CORVET subunit accumulating at endosomes (Figure 1B). Even though we did not determine Vps21 levels in comparison to Vps8, we reason that the endogenous amount of Vps21 is limiting to induce clustering, because the most efficient accumulation of MVBs also requires elevated Vps21 levels (Supplemental Figure S1; see below).

The fact that all CORVET subunits are not recruited to the Vps21 compartment could be caused by a poor assembly of the CORVET complex due to the Vps8 overproduction. We therefore verified, if the steady-state level of the CORVET complex was affected by isolating TAP-tagged Vps3 from strains with or without overexpressed Vps8. As shown in Figure 5D, Vps3 coprecipitated similar amounts of Vps8 from both strains. We noticed that the CORVET/HOPS subunit Vps11 is slightly reduced in the Vps8 overexpression strain. The significance of this observation will have to be addressed in future experiments. Because Vps3 and Vps8 interact only in the context of the CORVET complex (our unpublished observations), we conclude that Vps8 overproduction does not significantly affect the CORVET assembly dynamics and composition.

Based on the above observation, it is possible that the accumulation of Vps21 and Vps8 is the result of a tethering event, which may not require the entire CORVET complex. We therefore decided to analyze the localization of GFP-Vps21 in strains overexpressing Vps8, but lacking selected CORVET subunits that form the class C core (e.g., Vps11, Vps16, Vps18, or Vps33). To our surprise, GFP-Vps21 clearly accumulated in a single punctate structure in *vps11*Δ and *vps18*Δ, but not in *vps16*Δ cells (Figure 6A). The expression level of Vps21 was unaltered in the absence of Vps16 (Figure 6A, bottom). In *vps33*Δ cells, multiple GFP-Vps21 puncta were visible. It is possible that Vps33, which presumably interacts both with endosomal and vacuole SNAREs, supports the docking of endosomes, whereas Vps11 and Vps18 might be dispensable at this stage. GFP-tagged Vps8 behaves similarly to Vps21 (Figure 6B) and was also found in dot-like structures in *vps18*Δ cells and also in *vps16*Δ cells, in which Vps21 seems to be dispersed (Figure 6, A and B). When we analyzed the morphology of the structures accumulated in *vps11*Δ and *vps18*Δ cells by conventional EM, we frequently observed strongly docked vesicles (Figure 6C). However, the phenotype is rather complex because of the fragmentation of the vacuole. A detailed IEM study will need to clarify whether these structures contain Vps21 and Vps8 on their surface or have internal membranes. Nevertheless, our data suggest the Vps8-induced accumulation of Vps21 can occur in the absence of Vps11 and Vps18, suggesting an independent/early role of Vps8 within the CORVET complex during the fusion process.

We then asked whether we could reverse the Vps21 accumulation by coexpressing Vps8 with additional CORVET subunits (Figure 6D, top). We did not observe an effect on the Vps21 compartment if Vps3 was coexpressed with Vps8, though the vacuole fragmented under these conditions because of Vps3 overproduction (Figure 6D; Peplowska *et al.*, 2007). We then followed Vps21 in a diploid strain overexpressing Vps8 or the entire CORVET complex (F.Ahnert and C. Ungermann, unpublished observations). If all CORVET subunits were overexpressed, GFP-Vps21 did not accumulate, indicating that the endosomal clustering caused by Vps8 and Vps21 could be due to a retarded or not complete assembly of the CORVET complex that is necessary to complete the fusion between the tethered membranes and/or poor Vps8 and Vps21 release from LE (Figure 6D, bottom).

Vps8 Interacts with Vps21-GTP

Our data were indicating that Vps8 and Vps21 cooperate to achieve the clustering of MVBs. We therefore asked whether Vps8 can associate with purified Vps21. Initially, we used purified Vps8 from *E. coli* or yeast, but failed to detect specific interactions because of the inherent stickiness of Vps8 to the control beads (not shown). We therefore used a slightly indirect assay by using a lysate from cells overexpressing Vps8, which was added to glutathione (GSH) bead-bound glutathione S-transferase (GST)-Rabs. Vps8 was recovered efficiently with Vps21 but not Ypt7 (Figure 7A). The interaction was considerably stronger than any previously detected CORVET-Vps21 interaction (unpublished observations; Peplowska *et al.*, 2007). The reason for the poor nucleotide specificity could be due to the altered behavior of overproduced Vps8 as the purified CORVET has specificity to Vps21-GTP (Peplowska *et al.*, 2007). A similar observation has been obtained for the interaction of the homologous HOPS subunit Vps41 with Ypt7 (Brett *et al.*, 2008).

To further specify the nature of this binding, we tested the interaction of Vps8 with wild-type, GDP- (S21N) and GTP-locked (Q66L) forms of Vps21 using the Y2H assay (Haas *et al.*, 2005). As hypothesized, Vps8 interacts with Vps21 wild type and the GTP-locked, active Q66L mutant (Figure 7B, top). Initial mapping attempts indicate that the Vps21-GTP binding site resides in the C-terminal half of Vps8, whereas interaction with the class C subunit Vps11 requires the N-terminal portion of the protein (Figure 7B, bottom). Vps8 also binds the GTP-locked mutants of the Vps21 homologues Ypt52 and Ypt53 (Figure 7B, top), in agreement with earlier studies (Hama *et al.*, 1999). In contrast, the Vps21-GEF Vps9 interacts exclusively with the GDP-locked S21N mutant of Vps21 (Figure 7B, top). No interaction between Vps8, Vps9, and any of the Ypt7 forms was detected confirming that the CORVET complex acts with a set of Rab proteins different from those interacting with the HOPS complex. Vps3 binding to any Rab failed in this assay (not shown). Thus, our data suggest that Vps8 directly binds to Vps21-GTP and most likely correspond to the effector subunit of the CORVET complex.

To corroborate these findings in vivo, we followed the localization of overexpressed GFP-tagged Vps8 in response to Vps21-levels and its nucleotide state. In wild-type cells, Vps8 was found on some distinct puncta, but also showed a cytosolic repartition and some nuclear accumulation (as confirmed by DAPI staining, not shown), which increased in the absence of Vps21 (Figure 7C). When Vps21 levels were raised, Vps8 was confined to a single strong fluorescent dot, which corresponds to the clustered MVBs observed before (Figure 2). In agreement with our Y2H results, only the active, GTP-locked Vps21 form promoted this accumulation whereas an inactive, GDP-locked mutant failed to do so (Figure 7C).

To address the relation between Vps8, Vps21, and Vps3 in more detail, we finally focused on Vps8 localization. We previously showed that Vps21 requires Vps3 to induce clustering (Figure 1A) and that Vps8 localization requires Vps21-GTP (Figure 7C). However, we also noticed that the dot-like accumulation of Vps21 in absence of Vps16 was lost but not that of Vps8 (Figure 6, A and B). Even though these observations are difficult to interpret because of the strongly altered endocytic pathway, it suggested some differences in the behavior of the two proteins. We therefore analyzed

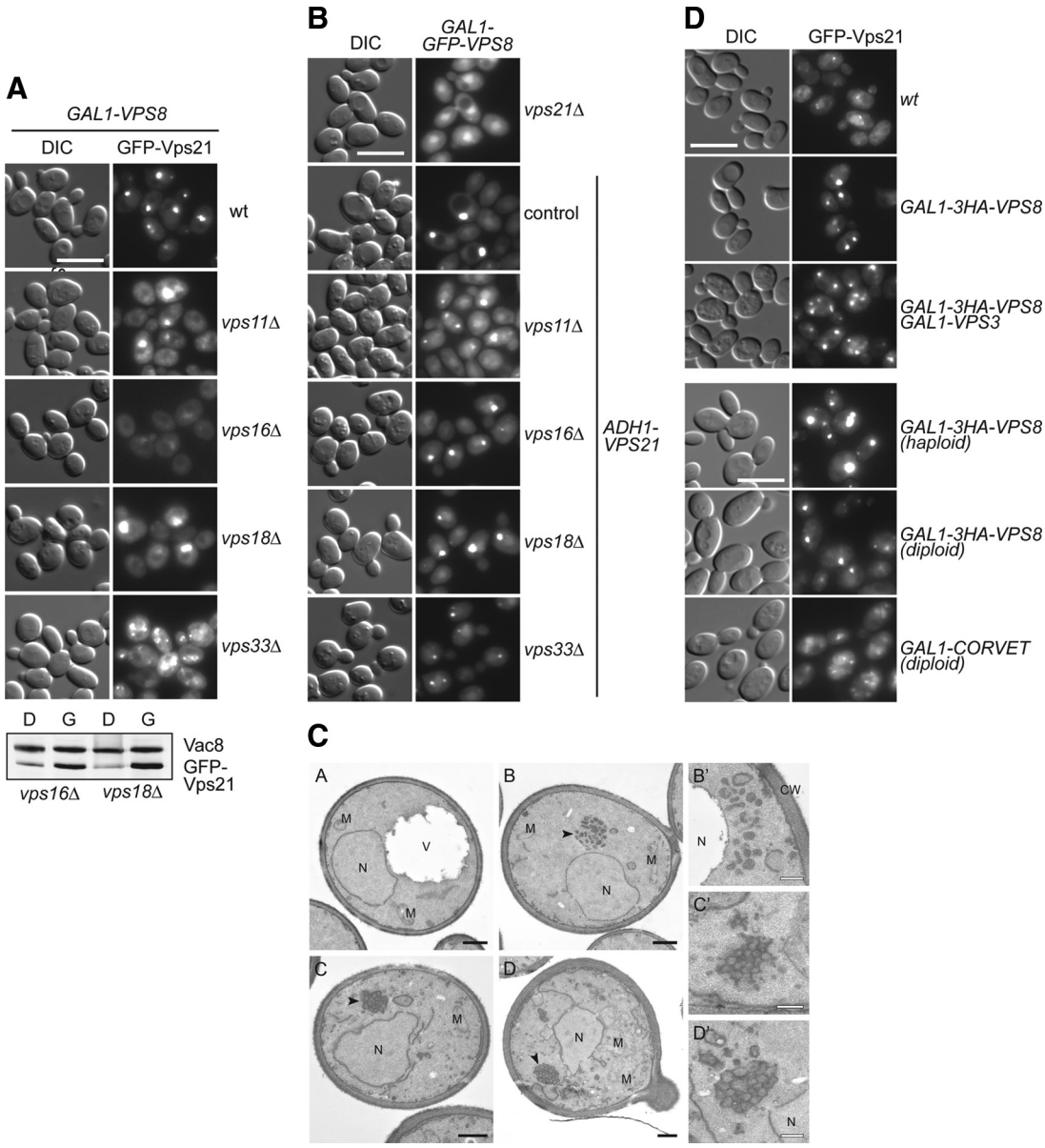

Figure 6. Role of the class C core proteins in the Vps21 localization to the LE clusters. (A and B) Localization of GFP-Vps21 (A) or GFP-Vps8 (B) in the indicated strains. Cells were analyzed by fluorescence microscopy as described in Figure 1A. Exposure times were identical for each strain. Size bar, 10 μm. The control of the expression levels is shown on the bottom of panel (A). Cell lysates were prepared from the indicated deletion strains expressing GFP-Vps21 and overexpressing Vps8, and proteins analyzed by SDS-PAGE followed by Western blotting. Vac8 is the loading control. (C) Ultrastructural analyses. Strains used for fluorescence microscopy in panel A: wild-type (image A), *GAL1-VPS8 GFP-VPS21* (image B), *GAL1-VPS8 GFP-VPS21 vps11*Δ (image C), and *GAL1-VPS8 GFP-VPS21 vps18*Δ (image D) were grown to exponential phase and embedded in Spurr's resin before being sectioned and imaged. The panels B′, C′, and D′ highlight the clusters of vesicles observed in the strains shown in images B, C, and D, respectively. V, vacuole; M, mitochondrion; N, nucleus. Black bar, 500 nm; white bar, 200 nm. (D) Localization of GFP-Vps21 in strains overexpressing Vps8 and Vps3 (top) or the entire CORVET (bottom). Wild-type, Vps8-overexpressing, and Vps8– and Vps3–co-overexpressing cells were analyzed by fluorescence microscopy. In the bottom panel, diploid cells overexpressing Vps8 or the entire CORVET complex are shown. Size bar, 10 μm.

GFP-tagged Vps8 in *vps3*Δ cells, which have large class D vacuoles positive for endosomal and vacuolar protein markers (Peplowska *et al.*, 2007). Here, we still observed dot-like structures in the vicinity of vacuoles, which strongly increased if Vps21 was also up-regulated (Figure 8A). Surprisingly, these structures were not stained by FM4-64 under these conditions and were often observed in some distance to the vacuole. We observe transient labeling of this compartment after short FM4-64 chase periods (not shown). This suggests that Vps8 requires Vps21 for its initial localization, most likely to EE. However, only in the presence of Vps3 clustering of Vps21-positive structures is induced, suggesting that the CORVET complex assembles after Vps8 has been recruited to membranes. Our data also suggest that Vps8 then remains on LE until they mature into MVBs. To directly test this, we localized GFP-tagged Vps8 in *vps4*Δ cells, which have an impaired MVB biogenesis. In wild-type cells, GFP-tagged Vps8 (here expressed from the strong *TEF1* promoter) is found on small punctate structures (Figure 8B), which were sometimes observed in close proximity

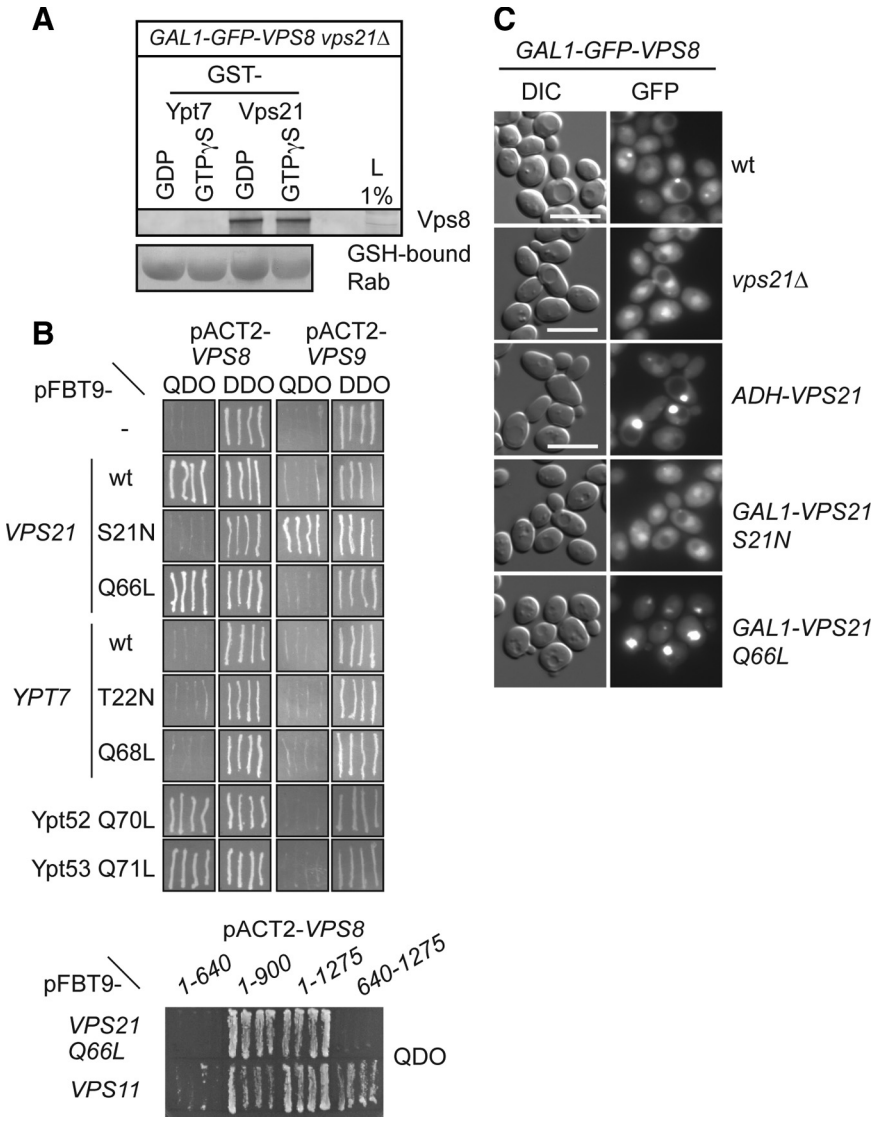

Figure 7. Recruitment of Vps8 to the LE depends on Vps21. (A) Interaction of Vps21 and Vps8 by pulldown experiments. Detergent lysates obtained from cells overexpressing GFP-Vps8 and lacking *VPS21* was applied to immobilized GST-Vps21 and GST-Ypt7, which were preloaded with the indicated nucleotide. Bound proteins were then eluted with EDTA and high salt concentration, TCA precipitated, and analyzed by Western blotting. Rab-GTPases were eluted by boiling beads in sample buffer and analyzed in the same way. (B) Top, analysis of the interaction between Vps21 and Vps8 by Y2H. The pACT2-Vps8 or pACT2-Vps9 plasmids were cotransformed with pFBT9 vectors carrying different forms of *VPS21* (wild-type, S21N, or Q66L), and *YPT7* (wild-type, T22N, or Q68L), or the activated alleles of *YPT52* (Q70L) and *YPT53* (Q71L). All transformants were restreaked onto QDO and DDO plates. Bottom, truncation analysis of Vps8. The pACT2-vectors expressing the indicated Vps8 truncations were cotransformed with pFBT9 vectors carrying either *VPS21 Q66L* or *VPS11*. Only the QDO plate is shown. (C) Fluorescence microscopy analysis of cells overexpressing GFP-tagged Vps8. Vps21 was either present at endogenous levels (wt), deleted (*vps21*Δ), or under the control of either the *ADH1* or the *GAL1* promoter (Vps21 S21N or Vps21 Q68L in *vps21*Δ cells). Images were collected as in Figure 1A. Size bar, 10 μm.

to the vacuole, and they were frequently stained by FM4-64. Such an accumulation was not detected for Vps3, which has a strong cytosolic pool (Peplowska *et al.*, 2007; not shown). In *vps4*Δ cells, Vps8 accumulated proximal to the vacuole. This phenotype was even further enhanced if combined with enhanced Vps21 levels (Figure 8B, bottom). Importantly, Vps8 was never found on the vacuolar rim under any conditions. We therefore suggest that Vps8 has to be removed before MVB fusion with the vacuole.

DISCUSSION

Our work highlights the cooperation of the Rab5 homolog Vps21 and Vps8 in tethering at the LE. We find that Vps21 strongly concentrates in LE structures upon overexpression of Vps8. Previous EM analyses have shown that the deletion of early endosomal fusion factors leads to the accumulation of 40-nm vesicles dispersed throughout the cytoplasm, which may be required to form and/or fuse with the LE (Cowles *et al.*, 1994; Becherer *et al.*, 1996; Burd *et al.*, 1996). The Vps21 compartment described here differs from the Vps21-positive structure observed in these previous studies. Our EM and IEM analyses have revealed an accumulation of larger vesicles (80–100 nm) with internal membranes that are organized in large clusters adjacent to the vacuole. This striking gathering of functional MVBs clearly differs from the dispersed vesicles accumulated in the mutants mentioned above. We ascribe this to LE tethering induced by Vps8 overexpression that still allows cargo sorting into the vacuole lumen, but results in poor retrieval of the Vps10-sorting receptor by the retromer (Figures 3 and 4). Previous studies have also reported MVB accumulation, though not to the extent reported here. The overproduction of Snx3 in mammalian cells leads to reduced endosomal transport and an accumulation of large MVBs with EE characteristics (Pons *et al.*, 2008). In addition, an enrichment of MVBs has been observed in yeast if Vps18 was impaired (Rieder and Emr, 1997), the Ypt7- and Vps33-interacting protein Ivy1 was overproduced (Lazar *et al.*, 2002) or if Vam3 was deleted (Darsow *et al.*, 1997). Although interference with Vps18, Vps33, Ypt7, or Vam3 could block the fusion of MVBs with vacuoles, Snx3 might directly affect the ESCRT machinery at the EE (Pons *et al.*, 2008). Because the MVB accumulation seems to be similar for Snx3 overproduction and Vps8–

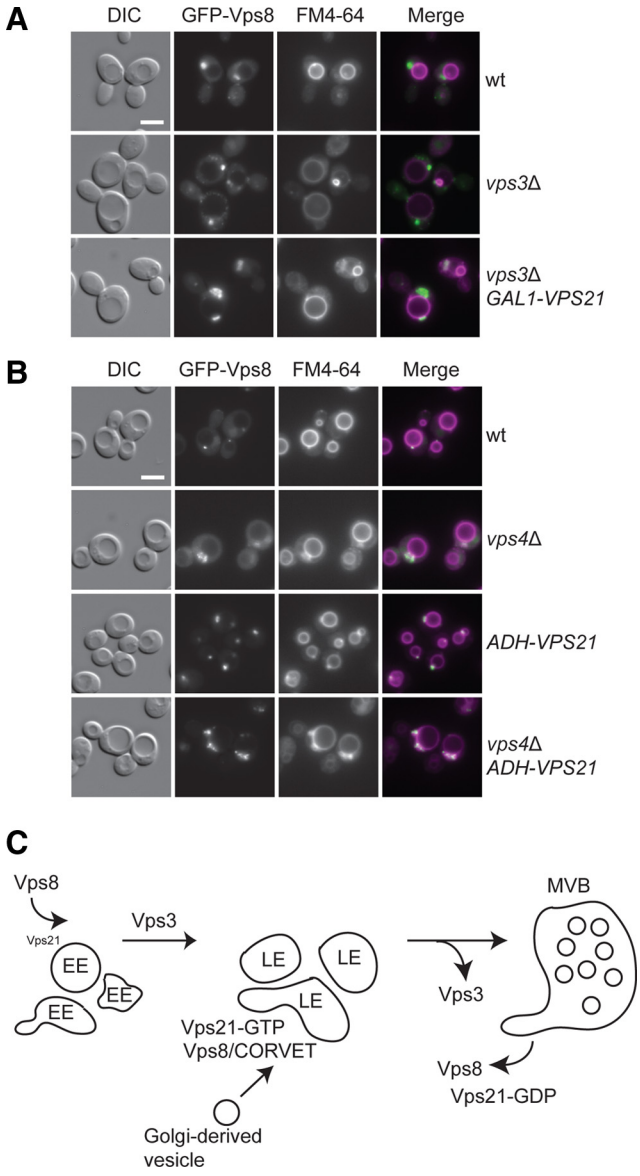

Figure 8. Vps8 recruitment to LE. (A) Localization of Vps8 in the absence of Vps3. BY strains expressing Vps8 from the *GAL1*-promoter were localized in wild-type and *vps3*Δ cells with or without *GAL1*-overproduced Vps21. Cells were analyzed by fluorescence microscopy as described in Figure 1A. Size bar, 5 μm. (B) Localization of Vps8 to LE. SEY6210 strains expressing Vps8 from the *TEF1* promoter were localized in wild-type and *vps4*Δ cells with or without *ADH1*-overproduced Vps21. Cells were analyzed by fluorescence microscopy as described in Figure 1A. Size bar, 5 μm. Similar results were obtained with BY strains. (C) Model of Vps8, Vps3, and Vps21 recruitment order during the maturation of endosomes. EE, early endosome; MVB, multivesicular body. See the text for details.

Vps21 overproduction, future studies should address how either protein (complex) affects maturation and consumption of MVBs.

Our data are consistent with the idea that the CORVET complex consists of subunits with distinct functions. It is required for the tethering of vesicles, a role that is most likely mediated by the Vps8 subunit and requires the interaction of this protein with the Rab5-homolog Vps21. This idea is supported by the interdependency of Vps21 and Vps8 in their LE localization and the GTP-dependent interaction between these two proteins (Figure 7). In addition to Vps8, Vps3, and Vps16 are the only CORVET subunits required for the clustering of GFP-Vps21 (Figures 1 and 6A). Interestingly, neither Vps3 nor Vps16 accumulate together with Vps8 and Vps21 under overexpression conditions, indicating that they might be involved in transient processes like Vps8-recruitment or Rab activation. Consistent with a putative GEF function, Vps3 binds to Vps21-GDP (Peplowska *et al.*, 2007), though the GEF activity has not yet been detected in vitro. Thus, the precise function of these subunits has to be investigated in more detail in the future.

In contrast to the deletions of *VPS3* and *VPS16*, we still observed GFP-Vps21 clustering in the absence of Vps11 or Vps18. This result indicates that these proteins could be dispensable for endosomal tethering and may be needed exclusively to promote fusion by controlling the SNARE protein assembly similarly to the homologous HOPS complex (Collins *et al.*, 2005; Starai *et al.*, 2008). In agreement with this idea, a thermosensitive mutant of Vps18 accumulates MVBs under restrictive conditions (Rieder and Emr, 1997), which could correspond to the clusters of vesicles observed in *vps11*Δ cells (Figures 6C). Nevertheless, the observed ultrastructural phenotypes of the *vps33*Δ and that of *vps11*Δ or *vps18*Δ mutant differ, and additional studies are necessary to clarify whether the Vps21- and Vps8-positive fluorescent structures also contain internal membranes.

How does the CORVET complex then operate? An initial amount of Vps21 is provided by the GEF Vps9 (Hama *et al.*, 1999) on EE to recruit effectors like Vac1/EEA1 (Tall *et al.*, 1999). This initial amount of Vps21-GTP could then be sufficient to recruit some Vps8 (Figure 8C), whereas Vps3 might be necessary to bind or provide additional Vps21-GTP. This could be a prerequisite of tethering at the endosomes, a step possibly necessary to guide the maturation of EE into LE and then into MVBs (Figure 8C). The CORVET complex–mediated tethering could be required for two different events. The first would be the fusion of EE and/or LE with additional endocytic or Golgi-derived vesicles. In fact, clusters are still observed in *vps9*Δ cells (Figure 1G). Several studies suggest that Vps8 is required for fusion of vesicles with the LE (Horazdovsky *et al.*, 1996; Woolford *et al.*, 1998; Srivastava *et al.*, 2000), and we previously showed that Vps8 can be efficiently copurified in the CORVET complex (Peplowska *et al.*, 2007). The second event where the CORVET complex could be of crucial relevance is the homotypic fusion of LE membranes. Yeast EE and LE are clusters of tubules and vesicles with a diameter of ~20–40 nm (Prescianotto-Baschong and Riezman, 1998; Griffith and Reggiori, 2009). In addition to form internal vesicles, these structures have to presumably fuse together to form a MVB, a compartment with a diameter of ~200–300 nm (Figure 5D; Griffith and Reggiori, 2009).

These functions of the CORVET complex at the LE may be retarded, when Vps8 and Vps21 are overexpressed because the tethering via these two proteins might occur independently of the assembled complex. The tethered vesicles very likely fuse and mature into MVBs, whereas newly formed vesicles are tethered to this structure at higher rates leading to the observed accumulation. This function could occur independently of Vps11 and Vps18 (Figure 6; Rieder and Emr, 1997). However, the complex of Vps21 and Vps8 may only function beyond tethering if the remaining CORVET subunits are present. Consequently, we observe a massive accumulation of MVBs, which in fact are smaller than the MVBs observed in wild-type cells (Figure 2). It is well possible that Vps8 release from the MVBs is necessary to allow successful endosomal maturation to occur and finally permit

fusion of MVBs with the vacuole, and the limiting CORVET subunits could be required at this stage. Indeed, Vps8 is found at the LE also in *vps4*Δ cells (Figure 8B). In agreement with such a model, overexpression of Vps8 and Vps21 did not lead to an enrichment of any additional HOPS or CORVET subunits at the LE (Figure 5A).

The observations reported here nicely complement and support observations made on other tethering systems. In the yeast secretory pathway, overexpression of the exocyst subunit Sec15, an effector protein of Sec4, leads to the formation of a cluster of secretory vesicles and a patch of Sec15 close to the plasma membrane that colocalizes with Sec4 (Salminen and Novick, 1989). The ability of Sec15 to form this patch depends on Sec4 and Sec2, a GEF for Sec4 (Salminen and Novick, 1989). In the endosomal system, Vps9 is the known Vps21 GEF, but is dispensable for the clustering of GFP-Vps21, whereas Vps3 is clearly required for Vps8 function in clustering of Vps21-positive structures, therefore suggesting that this protein could be a GEF. Potentially, Sec15 and its binding partner Sec10 are also required for the initial tethering of secretory vesicles (Salminen and Novick, 1989), whereas the remaining exocyst components assemble to promote fusion with the plasma membrane.

Recent observations on the reconstitution of early endosome fusion indicate that Rab5, tethers, and SNAREs cooperate in fusion (Ohya *et al*., 2009). However, because of the lack of mechanistic insights, tethering remains at present a poorly defined term. Our study suggests that the initial tethering activity on LE is confined to the interaction of Vps8 and Vps21-GTP, whereas the entire CORVET complex might act at a later stage to enhance tethering, bind other effectors, communicate with cargo, or assemble SNAREs in order to dictate fusion. A reconstitution of the initial tethering events and a detailed in vivo analysis will be necessary to reveal the exact order of events in LE maturation.

ACKNOWLEDGMENTS

We thank all members of our laboratories for fruitful discussions, Markus Babst (University of Utah, Salt Lake City, UT), Jeffrey Gerst, Michael Knop, and Tracy LaGrassa (Jones Day, Inc.) for strains and plasmids, and Angela Perz and Kathrin Auffarth for expert technical assistance. F.R. is supported by the Netherlands Organization for Health Research and Development (ZonMW-VIDI-917.76.329) and by the Utrecht University (High Potential grant). C.U. is supported by the SFB 431 and the Hans-Mühlenhoff foundation.

REFERENCES

Becherer, K. A., Rieder, S. E., Emr, S. D., and Jones, E. W. (1996). Novel syntaxin homologue, Pep12p, required for the sorting of lumenal hydrolases to the lysosome-like vacuole in yeast. Mol. Biol. Cell *7*, 579–594.

Brett, C. L., Plemel, R. L., Lobinger, B. T., Vignali, M., Fields, S., and Merz, A. J. (2008). Efficient termination of vacuolar Rab GTPase signaling requires coordinated action by a GAP and a protein kinase. J. Cell Biol. *182*, 1141–1151.

Burd, C. G., Mustol, P. A., Schu, P. V., and Emr, S. D. (1996). A yeast protein related to a mammalian Ras-binding protein, Vps9p, is required for localization of vacuolar proteins. Mol. Cell Biol. *16*, 2369–2377.

Burda, P., Padilla, S. M., Sarkar, S., and Emr, S. D. (2002). Retromer function in endosome-to-Golgi retrograde transport is regulated by the yeast Vps34 PtdIns 3-kinase. J. Cell Sci. *115*, 3889–3900.

Cabrera, M., Ostrowicz, C. W., Mari, M., LaGrassa, T. J., Reggiori, F., and Ungermann, C. (2009). Vps41 phosphorylation and the Rab Ypt7 control the targeting of the HOPS complex to endosome-vacuole fusion sites. Mol. Biol. Cell *20*, 1937–1948.

Collins, K. M., Thorngren, N. L., Fratti, R. A., and Wickner, W. T. (2005). Sec17p and HOPS, in distinct SNARE complexes, mediate SNARE complex disruption or assembly for fusion. EMBO J. *24*, 1775–1786.

Conibear, E., Cleck, J. N., and Stevens, T. H. (2003). Vps51p mediates the association of the GARP (Vps52/53/54) complex with the late Golgi t-SNARE Tlg1p. Mol. Biol. Cell *14*, 1610–1623.

Cowles, C. R., Emr, S. D., and Horazdovsky, B. F. (1994). Mutations in the VPS45 gene, a SEC1 homologue, result in vacuolar protein sorting defects and accumulation of membrane vesicles. J. Cell Sci. *107*, 3449–3459.

Darsow, T., Rieder, S. E., and Emr, S. D. (1997). A multispecificity syntaxin homologue, Vam3p, essential for autophagic and biosynthetic protein transport to the vacuole. J. Cell Biol. *138*, 517–529.

Drin, G., Morello, V., Casella, J. F., Gounon, P., and Antonny, B. (2008). Asymmetric tethering of flat and curved lipid membranes by a golgin. Science *320*, 670–673.

Gerrard, S. R., Bryant, N. J., and Stevens, T. H. (2000). VPS21 controls entry of endocytosed and biosynthetic proteins into the yeast prevacuolar compartment. Mol. Biol. Cell *11*, 613–626.

Griffith, J., Mari, M., De Maziere, A., and Reggiori, F. (2008). A cryosectioning procedure for the ultrastructural analysis and the immunogold labelling of yeast *Saccharomyces cerevisiae*. Traffic *9*, 1060–1072.

Griffith, J., and Reggiori, F. (2009). Ultrastructural analysis of nanogold-labeled endocytic compartments of yeast *Saccharomyces cerevisiae* using a cryo-sectioning procedure. J. Histochem. Cytochem. *57*, 801–809.

Grosshans, B. L., Ortiz, D., and Novick, P. (2006). Rabs and their effectors: achieving specificity in membrane traffic. Proc. Natl. Acad. Sci. USA *103*, 11821–11827.

Haas, A. K., Fuchs, E., Kopajtich, R., and Barr, F. A. (2005). A GTPase-activating protein controls Rab5 function in endocytic trafficking. Nat. Cell Biol. *7*, 887–893.

Hama, H., Tall, G. G., and Horazdovsky, B. F. (1999). Vps9p is a guanine nucleotide exchange factor involved in vesicle-mediated vacuolar protein transport. J. Biol. Chem. *274*, 15284–15291.

Horazdovsky, B. F., Cowles, C. R., Mustol, P., Holmes, M., and Emr, S. D. (1996). A novel RING finger protein, Vps8p, functionally interacts with the small GTPase, Vps21p, to facilitate soluble vacuolar protein localization. J. Biol. Chem. *271*, 33607–33615.

Janke, C., *et al*. (2004). A versatile toolbox for PCR-based tagging of yeast genes: new fluorescent proteins, more markers and promoter substitution cassettes. Yeast *21*, 947–962.

Kamena, F., Diefenbacher, M., Kilchert, C., Schwarz, H., and Spang, A. (2008). Ypt1p is essential for retrograde Golgi-ER transport and for Golgi maintenance in *S. cerevisiae*. J. Cell Sci. *121*, 1293–1302.

Kraynack, B. A., Chan, A., Rosenthal, E., Essid, M., Umansky, B., Waters, M. G., and Schmitt, H. D. (2005). Dsl1p, Tip20p, and the novel Dsl3(Sec39) protein are required for the stability of the Q/t-SNARE complex at the endoplasmic reticulum in yeast. Mol. Biol. Cell *16*, 3963–3977.

Lagrassa, T. J., and Ungermann, C. (2005). The vacuolar kinase Yck3 maintains organelle fragmentation by regulating the HOPS tethering complex. J. Cell Biol. *168*, 401–414.

Lazar, T., Scheglmann, D., and Gallwitz, D. (2002). A novel phospholipid-binding protein from the yeast *Saccharomyces cerevisiae* with dual binding specificities for the transport GTPase Ypt7p and the Sec1-related Vps33p. Eur. J. Cell Biol. *81*, 635–646.

Longtine, M. S., McKenzie, A., 3rd, Demarini, D. J., Shah, N. G., Wach, A., Brachat, A., Philippsen, P., and Pringle, J. R. (1998). Additional modules for versatile and economical PCR-based gene deletion and modification in *Saccharomyces cerevisiae*. Yeast *14*, 953–961.

Nickerson, D. P., Brett, C. L., and Merz, A. J. (2009). Vps-C complexes: gatekeepers of endolysosomal traffic. Curr. Opin. Cell Biol. *21*, 543–551.

Odorizzi, G., Babst, M., and Emr, S. D. (1998). Fab1p PtdIns(3)P 5-kinase function essential for protein sorting in the multivesicular body. Cell *95*, 847–858.

Ohya, T., Miaczynska, M., Coskun, U., Lommer, B., Runge, A., Drechsel, D., Kalaidzidis, Y., and Zerial, M. (2009). Reconstitution of Rab- and SNARE-dependent membrane fusion by synthetic endosomes. Nature *459*, 1091–1097.

Ostrowicz, C. W., Meiringer, C. T., and Ungermann, C. (2008). Yeast vacuole fusion: a model system for eukaryotic endomembrane dynamics. Autophagy *4*, 5–19.

Peplowska, K., Markgraf, D. F., Ostrowicz, C. W., Bange, G., and Ungermann, C. (2007). The CORVET tethering complex interacts with the yeast Rab5 homolog Vps21 and is involved in endo-lysosomal biogenesis. Dev. Cell *12*, 739–750.

Peterson, M. R., Burd, C. G., and Emr, S. D. (1999). Vac1p coordinates Rab and phosphatidylinositol 3-kinase signaling in Vps45p-dependent vesicle docking/fusion at the endosome. Curr. Biol. *9*, 159–162.

Piper, R. C., Cooper, A. A., Yang, H., and Stevens, T. H. (1995). VPS27 controls vacuolar and endocytic traffic through a prevacuolar compartment in *Saccharomyces cerevisiae*. J. Cell Biol. *131*, 603–617.

Pons, V., Luyet, P. P., Morel, E., Abrami, L., van der Goot, F. G., Parton, R. G., and Gruenberg, J. (2008). Hrs and SNX3 functions in sorting and membrane invagination within multivesicular bodies. PLoS Biol. *6*, 1942–1956.

Prescianotto-Baschong, C., and Riezman, H. (1998). Morphology of the yeast endocytic pathway. Mol. Biol. Cell *9*, 173–189.

Price, A., Seals, D., Wickner, W., and Ungermann, C. (2000a). The docking stage of yeast vacuole fusion requires the transfer of proteins from a *cis*-SNARE complex to a Rab/Ypt protein. J. Cell Biol. *148*, 1231–1238.

Price, A., Wickner, W., and Ungermann, C. (2000b). Proteins needed for vesicle budding from the golgi complex are also required for the docking step of homotypic vacuole fusion. J. Cell Biol. *148*, 1223–1230.

Puig, O., Rutz, B., Luukkonen, B. G., Kandels-Lewis, S., Bragado-Nilsson, E., and Seraphin, B. (1998). New constructs and strategies for efficient PCR-based gene manipulations in yeast. Yeast *14*, 1139–1146.

Raymond, C. K., Howald-Stevenson, I., Vater, C. A., and Stevens, T. H. (1992). Morphological classification of the yeast vacuolar protein sorting mutants: evidence for a prevacuolar compartment in class E vps mutants. Mol. Biol. Cell *3*, 1389–1402.

Rieder, S. E., and Emr, S. D. (1997). A novel RING finger protein complex essential for a late step in protein transport to the yeast vacuole. Mol. Biol. Cell *8*, 2307–2327.

Rojas, R., van Vlijmen, T., Mardones, G. A., Prabhu, Y., Rojas, A. L., Mohammed, S., Heck, A. J., Raposo, G., van der Sluijs, P., and Bonifacino, J. S. (2008). Regulation of retromer recruitment to endosomes by sequential action of Rab5 and Rab7. J. Cell Biol. *183*, 513–526.

Salminen, A., and Novick, P. J. (1989). The Sec15 protein responds to the function of the GTP binding protein, Sec4, to control vesicular traffic in yeast. J. Cell Biol. *109*, 1023–1036.

Seaman, M. N., Harbour, M. E., Tattersall, D., Read, E., and Bright, N. (2009). Membrane recruitment of the cargo-selective retromer subcomplex is catalysed by the small GTPase Rab7 and inhibited by the Rab-GAP TBC1D5. J. Cell Sci. *122*, 2371–2382.

Shorter, J., Watson, R., Giannakou, M. E., Clarke, M., Warren, G., and Barr, F. A. (1999). GRASP55, a second mammalian GRASP protein involved in the stacking of Golgi cisternae in a cell-free system. EMBO J. *18*, 4949–4960.

Srivastava, A., Woolford, C. A., and Jones, E. W. (2000). Pep3p/Pep5p complex: a putative docking factor at multiple steps of vesicular transport to the vacuole of *Saccharomyces cerevisiae*. Genetics *156*, 105–122.

Starai, V. J., Hickey, C. M., and Wickner, W. (2008). HOPS proofreads the trans-SNARE complex for yeast vacuole fusion. Mol. Biol. Cell *19*, 2500–2508.

Tall, G. G., Hama, H., DeWald, D. B., and Horazdovsky, B. F. (1999). The phosphatidylinositol 3-phosphate binding protein Vac1p interacts with a Rab GTPase and a Sec1p homologue to facilitate vesicle-mediated vacuolar protein sorting. Mol. Biol. Cell *10*, 1873–1889.

Wang, W., Sacher, M., and Ferro-Novick, S. (2000). TRAPP stimulates guanine nucleotide exchange on Ypt1p. J. Cell Biol. *151*, 289–296.

Whyte, J. R., and Munro, S. (2002). Vesicle tethering complexes in membrane traffic. J. Cell Sci. *115*, 2627–2637.

Woolford, C. A., Bounoutas, G. S., Frew, S. E., and Jones, E. W. (1998). Genetic interaction with *vps8-200* allows partial suppression of the vestigial vacuole phenotype caused by a *pep5* mutation in *Saccharomyces cerevisiae*. Genetics *148*, 71–83.

Wurmser, A. E., Sato, T. K., and Emr, S. D. (2000). New component of the vacuolar class C-Vps complex couples nucleotide exchange on the ypt7 GTPase to SNARE-dependent docking and fusion. J. Cell Biol. *151*, 551–562.